3rd EUROPEAN CONFERENCE
ON UNDERWATER ACOUSTICS
Heraklion, Crete, Greece
24-28 June, 1996

Bubble detection using low amplitude multiple acoustic techniques

T. G. Leighton, A. D. Phelps and D. G. Ramble

Institute of Sound and Vibration Research, University of Southampton, Highfield, Southampton SO17 1BJ, UK

There exists a range of acoustic techniques for characterising bubble populations within liquids. Each technique has limitations, and complete characterisation of a population requires the sequential or simultaneous use of several, so that the limitations of each find compensation in the others. Here, nine techniques are deployed using one experimental rig, and compared to determine how accurately and rapidly they can characterise injected, rising bubbles. The study was carried out using relatively low-amplitude acoustic fields to drive the bubble, which is desirable to minimise the invasiveness of the technique.

1. INTRODUCTION

Bubble detection, necessary in numerous practical applications [1], is usually achieved through use of a single technique [2]. Each of these has limitations, and this paper investigates how they may be used together to better measure a bubble population. Some exploit the bubble pulsation resonance. In water with ambient pressure $p0$, an air bubble of radius $R0>\sim10$ μm has a well-defined resonance frequency $f0=\omega0/2\pi\approx0.01(\sqrt{p0})/R0$, and pulsates as a lightly-damped oscillator: On entrainment the pulsations generate an exponentially-decaying sinusoid at the natural frequency, which can give the bubble size [3]. Strong scattering of an acoustic signal at a given 'pump' frequency ω_p, incident upon an unknown bubble population, might occur from resonant bubbles, or from bubbles much larger than resonance which, though not coupling to the field through pulsation, simply present a large target for geometric scattering [2] (an effect which, though creating an ambiguity above, is exploited later). Unlike the bubble-mediated scattering of ω_p, that of the second ($2\omega_p$) and higher harmonics is a global maximum at resonance [4]. Global maxima at resonance also occur when a bubble is insonated, not only at ω_p (which, being of the same order as the resonance, drives it into pulsation), but also by an 'imaging' signal [5] at a much higher frequency, ω_i: In this case a range

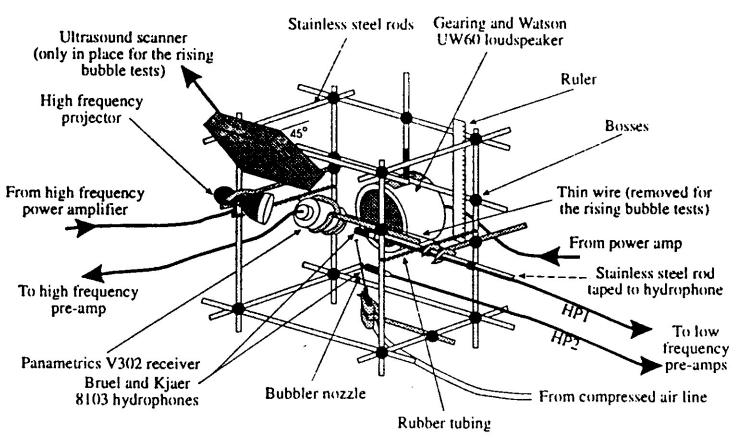

Fig. 1. Schematic of apparatus mounted in cage. For these rising bubble tests the thin wire in cage centre is removed.

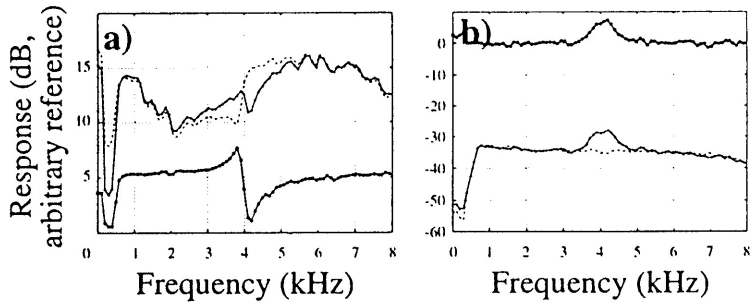

Fig. 2 Response (voltage transfer modulus) for 1-8 kHz broadband insonation from a) HP1 and b) heterodyned high-frequency signals. Resolution: 98 Hz. Key:(- - -)≡no bubbles; (—+—) ≡bubbles present; (—•—)≡ratio 'bubbles present':'no bubbles'. Data points at symbols.

of signals arising from combinations of ω_i with ω_p and its harmonics when ω_p is close to the resonance [6]. Though signals at ω_p, $2\omega_p$, $\omega_i \pm \omega_p$, $\omega_i \pm \omega_p/2$ and geometrical scattering have individually been used to size bubbles, here the principle is to use them simultaneously to compare and compensate for their limitations and off-resonance effects.

2. METHOD

The transducers are held in rigid 'cage' (Fig. 1) which is placed at depth 0.15 m in a 1.8 m x 1.2 m x 1.2 m deep vibration isolated glass reinforced plastic tank. The method is detailed elsewhere [7]. Bubbles, injected at 29 cm depth, emit a passive signal which is monitored on hydrophone HP2 (Bruel and Kjaer 8103). The bubbles rise into the field of an underwater loudspeaker (Gearing and Watson UW60) which drives them with the 'pump' signal: either a broadband (1-8 kHz bandlimited) pump signal; or with tone bursts, spaced 1.6 s apart and of 0.2 s duration (240 Pa acoustic pressure amplitude at the bubble), the frequency in each burst being 100 Hz greater than its predecessor. Initial broadband insonation allows bubble resonances to be rapidly (if roughly) estimated, reducing the frequency range which the more finely-resolving tone-burst increments must more slowly cover. A second B&K 8103 hydrophone (HP1), 1 cm from the needle tip, monitors the audio-frequency signals by the rising bubbles. Simultaneously the bubble receives the 'imaging' signal ($\omega_i/2\pi$=1.134 MHz) from a Therasonic 1030 (EMS) generator, and, with the beamplots intersecting at 15 cm depth over a 1.2 cm^3 volume, a Panametrics V302 receiver detects the combination-frequency signal before it is heterodyned with the Therasonic signal. The data is averaged over the 10^4 samples collected in each increment. A Hitachi EUB-26E 3.5 MHz ultrasound scanner, mounted in the cage, gave M- and B-mode images of the rising bubbles. Atmospheric pressure was 0.1003 MPa. After rising, bubbles are collected on a glass plate for photography.

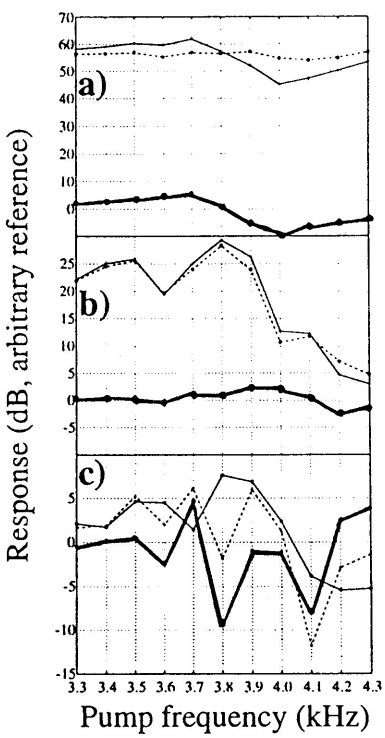

Fig. 3 Response at a) ω_p, b) $2\omega_p$, c) $\omega_p/2$ in the HP1 signal. Key as for Fig. 2, with (o) at 'no bubble' data points.

3. RESULTS

The scatter of the broadband sound field by the bubble stream, measured using HP1 (Fig. 2a) indicates that the ratio of the

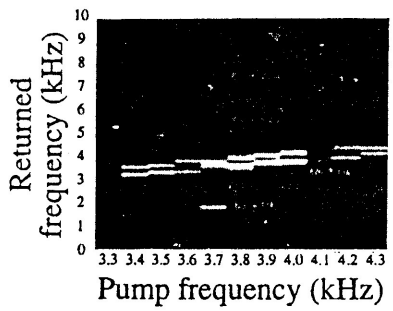

Fig. 4 Greyscale histogram showing heterodyned V302 received signal for each discrete setting of the pump frequency (100 Hz increments). Light shades indicate strong signal. Signals at $\omega_i \pm \omega_p/2$, $\omega_i \pm \omega_p$, $\omega_i \pm 3\omega_p/2$ *and* $\omega_i \pm 2\omega_p$ *are indicated.*

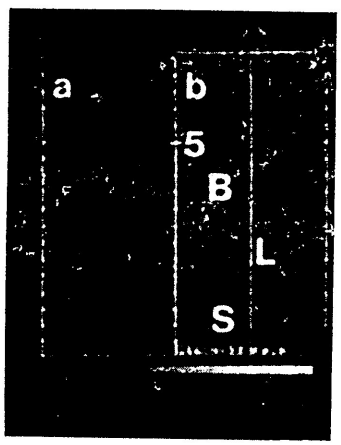

Fig. 5 a) M-mode (1 s sweep) and b) B-mode images from Hitachi ultrasound scanner. In 'b' a bubble (B), UW60 speaker (S), the 5 cm marker from transducer faceplate (at top of image) and the line (L, occurrence of an image in which defines the M-mode image) are indicated.

'bubbles present' signal to the 'no bubbles' signal (the bubble-mediated "amplification") exhibits a through-resonance effect, centred around 4±0.1 kHz. In Fig. 2b the heterodyned signal from the high frequency receiver (with an 800 Hz high pass filter to remove low-frequency Doppler components) shows bubble-mediated change centred at 4.2±0.3 kHz. Having thus rapidly found the region of interest (3.3 to 4.3 kHz), the pump sound field is incremented in this range in steps of 100 Hz, at a pressure amplitude of 240 Pa (0-pk). Fig. 3 shows the results of analysis of the signal recorded by hydrophone HP1. In Fig. 3a the scattering of the fundamental frequency ω_p gives $f_0 \approx$ 3850±20 Hz. The second harmonic $2\omega_p$ neither immediately indicates a distribution around a single bubble size (Fig. 3b) nor accurately what that size might be ($f_0 \approx$3.8±0.15 kHz). The results at $\omega_p/2$ are also unclear (Fig. 3c). During the same single pass from 3.2 to 4.4 kHz as provided the data for Fig. 3, data was taken from the combination frequency technique using the Panametrics V302 receiver, and the results are shown in Fig. 4, as a greyscale plot showing the received, heterodyned spectrum as a function of the pump frequency (this, on the horizontal axis, indicating not a continuum but the 12 settings of the pump frequency, since the latter was incremented in 100 Hz steps). In the greyscale plot, signals at $\omega_i \pm \omega_p$, $\omega_i \pm 2\omega_p$ and $\omega_i \pm \omega_p/2$ are labelled. It is not possible to determine the size of bubbles using the $\omega_i \pm \omega_p$ plot, which suggests a broad range of sizes are present over more than a kHz range. The clearest indication of resonance is that only for the pump frequency setting of 3.7 kHz does structure in the heterodyned spectrum at frequencies which are multiples of $\omega_p/2$ (i.e. $\omega_p/2$, ω_p, and $3\omega_p/2$, and $2\omega_p$) occur. All other peaks do not correspond to multiples of ω_p. Fig. 5 shows both the a) M- and b) B-mode images obtained using the Hitachi ultrasound scanner, the section shown being a slice at 45° to vertical (Fig. 1). The bubble (labelled B) can be located in Fig. 5b (near-field is at top of image), which also images the loudspeaker (S) and part of the cage. Images which intersect the vertical line (L) in 1 s are plotted in Fig. 5a: almost 19 bubbles pass through the beam in that time, with rise speed (from the image, assuming local rectilinear bubble motion in the 45° beam orientation) of 20±2 cm/s, covering an implied 0.87-1.13 mm radii range [7, 8].

4. DISCUSSION

The bubble sizes inferred from the various signals are summarised in Table 3. Since the 1 s broadband test (Cols. 2,3) is performed at a different time to the incremented tone test (Cols. 4-10), they sample different bubble populations [7]. The Gabor technique can log all bubbles which are injected, and indicates variability in the population commensurate with the results of

Table 3 [7]. Only the simultaneous occurrence of the structure at $\omega_i \pm \omega_p/2$, $\omega_i \pm 3\omega_p/2$, and $\omega_i \pm 2\omega_p$ allows accurate active characterisation, giving the resonance of 3.70±0.05 kHz, the limits of accuracy having been *chosen* by the imposition of a 240 Pa pump signal amplitude to ensure a 100 Hz increment, large enough to cover the required frequency range within the chosen time, which will not undercount.

Table 3. Resonances and calculated radii for populations with broadband and tonal pump signals.

	← Broadband →			← Incremented pump tonebursts →					
Column 1	Col. 2	Col. 3	Col. 4	Col. 5	Col. 6	Col. 7	Col. 8	Col. 9	Col. 10
Signal:	ω_p	$\omega_i \pm \omega_p$	ω_p	$2\omega_p$	$\omega_p/2$	$\omega_i \pm \omega_p$	$\omega_i \pm \omega_p/2$	$\omega_i \pm 2\omega_p$	$\omega_i \pm 3\omega_p/2$
Distribution indicated	Narrow (Fig 2a)	Broad (Fig 2b)	Narrow (Fig 3a)	Fig 3b	Bimodal (Fig 3c)	Broad (Fig 4)	Narrow (Fig 4)	Narrow (Fig 4)	Narrow (Fig 4)
Resonance f_0 /kHz	4 ±0.1	4.2 ±0.3	3.85 ±0.1	3.9 ±0.2	3.9 ±0.2	3.8 ±0.5	3.7 ±0.05	3.7 ±0.05	3.7 ±0.05
$\frac{R_0}{\mu m} \approx \frac{p_0^{1/2}}{100 f_0}$	800 ±20	760 ±50	830 ±22	840 ±33	820 ±42	840 ±110	862 ±12	862 ±12	862 ±12

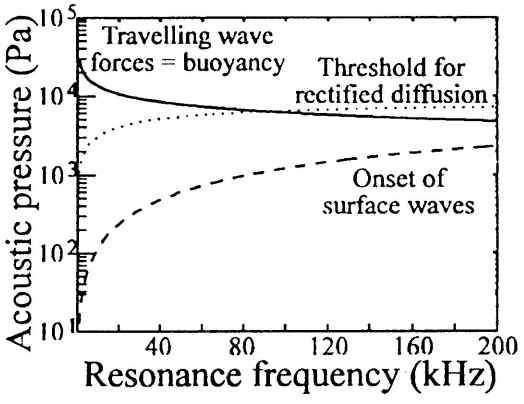

Fig. 6. Plot demonstrating the invasiveness of acoustic techniques, showing: thresholds for surface waves (dashed), & rectified diffusion (dotted); and equivalence of radiation force with buoyancy (unbroken).

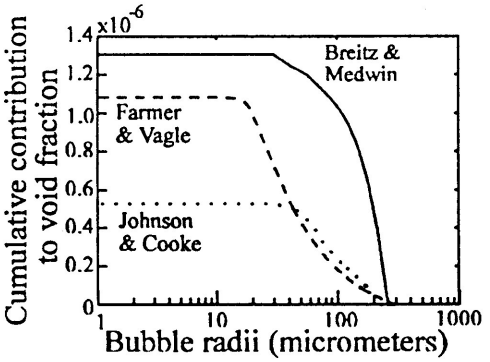

Fig. 7. The cumulative contribution (of estimates of the bubble radii) to the eventual void fraction from integration of the oceanic bubble population data of Breitz & Medwin ([12], unbroken), Farmer & Vagel ([13, dashed) and Johnson & Cooke ([14], dotted).

The 240 Pa pump signal amplitude is relatively low for underwater acoustics applications, a consideration if a technique is to be minimally invasive. To examine this the thresholds for $\omega_i \pm \omega_p/2$ (calculated from that for surface wave generation [7]), and for inducing bubble growth in resonant bubbles by rectified diffusion [1] (after Eller [9]) was calculated in the range 0-200 kHz. Though the radiation force from a travelling wave acoustic field, which may induce bubble translations, has no threshold, an estimate of its importance can be found by calculating [1, 10] that acoustic pressure amplitude at which the force equals that of buoyancy. These are shown in Fig. 6. Clearly detection using $\omega_i \pm \omega_p/2$ at the threshold amplitude is unlikely to be invasive in this respect, but it would be advisable for workers to record the acoustic pressure amplitudes *at the bubble* when using any acoustic technique.

The calculation was made up to 200 kHz since integration [11] of bubble size densities from three surveys yields total gas void fractions (as shown in Fig. 7) of 1.3×10^{-6} [12], 1.1×10^{-6} [13], and, from the only optical survey of the three, 0.5×10^{-6} [14]. To measure 95% of the void fraction each survey did in

fact measure, the minimum bubble radius each survey would have to measure would be 43 μm for both [12] and [14], and 18 μm for [13]. To measure this lowest estimate of the minimum radius would require a resonant pump frequency of 200 kHz.

5. CONCLUSIONS

Broadband insonation rapidly indicates the range over which bubble resonances may occur, reducing the time required for tonal incrementation. Best resolution and population sampling was achieved using the Gabor technique, though this operates only on entrainment. With the pump signal amplitude of 240 Pa used here, the occurrence of simultaneous structure in the combination-frequency spectrum most accurately indicated the resonance range of rising bubbles, the limits of accuracy being a chosen compromise with speed of the examination. Little invasiveness is expected with the low amplitudes used here.

Acknowledgements Our thanks to EPSRC (ref. GR/H 79815) and to PR White.

REFERENCES

[1] T.G. Leighton, *The Acoustic Bubble*, Academic Press, London, 1994, pp. 216-7, 442, 533, 546-7, 563-6; 198-203; 379-407; 341-67 234-43; 295-98; 439-64

[2] T.G. Leighton, *Acoustic Bubble Detection. I. The detection of stable gas bodies*, Environmental Engineering **7**, (1994) 9-16

[3] M. Minnaert, *On musical air-bubbles and the sounds of running water*, Phil. Mag. **16** (1933), 235-248

[4] D.L. Miller, *Ultrasonic detection of resonant cavitation bubbles in a flow tube by their second harmonic emissions*, Ultrasonics **19** (1981) 217-24

[5] Newhouse V.L and Shankar P.M. *Bubble size measurement using the nonlinear mixing of two frequencies*, J. Acoust. Soc. Am. **75** (1984) 1473-7

[6] A.D. Phelps and T.G. Leighton, *High resolution bubble sizing through detection of the subharmonic response with a two frequency excitation technique*. JASA In press. (1996)

[7] T.G. Leighton, D.G. Ramble & A.D. Phelps, *Comparison of the abilities of multiple acoustic techniques for bubble detection*, Proc. Inst. of Acoustics **17** (8), (1995) 149-160

[8] R. Clift, J.R. Grace, & M.E. Weber. *Bubbles, Drops and Particles.* Academic Press, 1978

[9] A I. Eller, *Growth of bubbles by rectified diffusion*, J Acoust Soc Am. **46** (1969) 1246-50

[10] W.T. Coakley & W.L. Nyborg. *Chapter II: Cavitation; dynamics of gas bubbles; applications* in F. Fry Ed., *Ultrasound: its applications on medicine and biology* Elsevier, Amsterdam, 1978 ,Part 1 pp. 77-159

[11] A.D. Phelps, *Characterisation of the subharmonic response of a resonant bubble using a two frequency technique*, PhD, Southampton University, 1995

[12] N. Breitz & H. Medwin, *Instrumentation for in-situ acoustical measurements of bubble spectra under breaking waves*, J. Acoust. Soc. Am. **86** (1989) 739-43

[13] D.M. Farmer & S. Vagle, *Waveguide propagation of ambient sound in the ocean-surface bubble layer*, J. Acoust. Soc. Am. **86** (1989) 1897-1908

[14] B.D. Johnson & R.C. Cooke, *Bubble populations and spectra in coastal waters; a photographic approach*, J. Geophys. Res. **84** (C7) (1979) 3761-6